ELSEVIER

Surface Science 482–485 (2001) 1130–1134

SURFACE SCIENCE

www.elsevier.nl/locate/susc

Potential drop along carbon nanotube devices with current flow

N. Mingo [a,b,*], J. Han [b], M.P. Anantram [b], L. Yang [b]

[a] *Department of Physics and Astronomy, North Carolina University, Chapel Hill, NC, USA*
[b] *NASA-Ames Research Center, Mailstop T27A-1, Moffett Field, CA 94035, USA*

Abstract

Electronic transport in carbon nanotube devices is calculated self-consistently and characterized by potential profile, using a non-equilibrium Green function approach. We study the potential drop along structures with two types of scatters: randomly disordered, and nanotube 'heterojunctions'. While perfectly conducting tubes have a flat potential along the tube axis, all the potential drop taking place at the contacts, highly disordered tubes display a linear potential drop profile, showing diffusive conducting behavior. For a heterojunction in which three metallic tubes are connected by topological defects, the potential drop takes place also at the defect located interfaces. Reference is also made to experimental results and applications. © 2001 Elsevier Science B.V. All rights reserved.

Keywords: Green's function methods; Computer simulations; Conductivity; Electrical transport (conductivity, resistivity, mobility, etc.); Surface electronic phenomena (work function, surface potential, surface states, etc.); Carbon

1. Introduction

A carbon nanotube is viewed as a hollow cylinder, constructed by rolling up a graphene sheet along a lattice vector (n, m). It is metallic if mod$(n - m, 3) = 0$, and otherwise it is semi-conducting and typically has a 1 eV band gap for 1 nm tube diameter [1]. Nanotube devices such as transistors [2] and junction diodes [3] have been demonstrated experimentally. Theoretically, despite calculations exist for transmission vs. energy curves of nanotube devices [4], these are not enough to predict the I–V characteristics of nanotube electronic devices. Proper self-consistent calculations, taking into account the non-equilibrium electron distribution have been done for linear chains [5], but not for carbon nanotubes.

For electronic transport of nanotube devices carrying the current flow, a self-consistent calculation has to be carried out to establish the potential profile along the tube axis. In this work, we formulate a self-consistent calculation using a non-equilibrium Green function approach specific for versatile nanotube devices. The calculations are conducted for two typical nanotube device architectures. One is single nanotube devices to which structural disorder is introduced. The other is a nanotube heterojunction in which tubes with different helicities or (n, m) are connected by topological defects. The atomic structures are obtained using the molecular dynamics method of Han [6].

* Corresponding author. Address: NASA-Ames Research Center, Mailstop T27A-1, Moffett Field, CA 94035, USA. Tel.: +1-650-604-1776; fax: +1-650-604-3957.
E-mail address: mingo@nas.nasa.gov (N. Mingo).

0039-6028/01/$ - see front matter © 2001 Elsevier Science B.V. All rights reserved.
PII: S0039-6028(01)00734-8

An extensive study of different heterojunctions and their conducting properties will be published elsewhere [7]. The calculated potential profile results are used to understand electronic transport properties in nanotube transistors and heterojunction diodes.

2. Theoretical method

Electronic structure of a system is treated within a linear combination of atomic orbitals (LCAO) framework. The system is linked to two semi-infinite tubes acting as emitter and collector. This is taken into account in the Hamiltonian by adding a self-energy part such that $H = H_0 + \Sigma(E)$ [8], where H_0 is of the system isolated from the emitter and collector. The matrix $\Sigma(E)$ is calculated by the 'decimation technique' of Guinea et al. [8]. The normal equilibrium local density of states is given by

$$\rho^{\mathrm{tot}} = \frac{1}{\pi}\mathrm{Im}\, G \tag{1}$$

In the absence of current this is used to obtain the total charges of the system by integrating in energy. If a bias is applied between the emitter and collector, however, two Fermi levels (rather than one) are defined in the system, and the total charge at 0 temperature is given by

$$q_{ij} = \int_{-\infty}^{E_{\mathrm{f}}(\mathrm{coll})} \rho_{ij}^{\mathrm{tot}}(E)\,\mathrm{d}E + \int_{E_{\mathrm{f}}(\mathrm{coll})}^{E_{\mathrm{f}}(\mathrm{em})} \rho_{ij}^{\mathrm{trans}}(E)\,\mathrm{d}E \tag{2}$$

Here the transmitted density ρ^{trans} corresponds to the density of states that enter from the emitter. In terms of Green functions, the matrix for the transmitted l.d.o.s. at ring i of the tube is

$$\underline{\rho_i}^{\mathrm{trans}} = \mathbf{D}_i \underline{\rho_i^0} \mathbf{D}_i^{\dagger} \tag{3}$$

where

$$\mathbf{D}_i = (\mathbf{I} - (g_{i,i}\mathbf{T}_{i,i+1}\mathbf{g}_{i+1,i+1}\mathbf{T}_{i+1,i}))^{-1}, \quad \underline{\rho_i^0} = \frac{1}{\pi}\mathrm{Im}\,\mathbf{g}_i \tag{4}$$

and $\mathbf{g}_{i,i}$ is the Green function matrix corresponding to layer i of the system when layers i and $i+1$ are uncoupled. $\mathbf{T}$ is the Hamiltonian matrix coupling layer i to $i+1$. Eqs. (3) and (4) are matrix generalization of the corresponding expressions in Ref. [5].

In the case of perfect transmission through the tube (perfect translational symmetry), $\rho^{\mathrm{trans}} = 0.5\rho^{\mathrm{tot}}$. In the limiting case of zero transmission, at the emitter side we have $\rho^{\mathrm{trans}} = \rho^{\mathrm{tot}}$, and at the collector side $\rho^{\mathrm{trans}} = 0$. In general, the transmitted l.d.o.s. as a function of energy is non-trivial for heterostructures, and has to be calculated from Eq. (3). The external potential is included in the Hamiltonian as $\mathbf{H}' = \mathbf{H} + \mathbf{V}$, with

$$V_{ij} = \sum_{kl} M_{ijkl} q_{kl} \tag{5}$$

Exchange and correlation terms can be included in the LCAO Hamiltonian in the way explained in Refs. [9,10]. In this work, we further simplify the potential to be a diagonal matrix, so that

$$V_{ij} = \sum_{k} \delta_{ij} M_{jk} q_{kk} \tag{6}$$

where the electrostatic matrix between orbitals i and j is calculated as in Ref. [10]. The self-consistent potential is then iteratively computed until it satisfies $\mathbf{V}^{\mathrm{sc}} = \mathbf{M}\mathbf{q}(\mathbf{V}^{\mathrm{sc}})$, where $\mathbf{q}(\mathbf{V})$ is calculated according to Eq. (2).

3. Results

We first qualitatively discuss the self-consistent potential for single tube and heterojunction devices between two infinite metallic planes under applied bias. In the absence of disorder or perfect tube structures, if bias is applied between the electrodes joined by the nanotube, the potential profile is flat along the nanotube with an immediate potential drop at the contacts. This is because $\rho^{\mathrm{trans}} = 0.5\rho^{\mathrm{tot}}$ so that raising E_{f} (emitter) by $V/2$ and lowering E_{f} (collector) by $V/2$ do not change the local onsite charge obtained from Eq. (2). However, when disorder or other kind of barriers for electron transmission are present in nanotubes, $\rho^{\mathrm{trans}} > 0.5\rho^{\mathrm{tot}}$ at the emitter side and $\rho^{\mathrm{trans}} < 0.5\rho^{\mathrm{tot}}$ at the collector side. This implies that more charges tend to accumulate on the emitter side of the barrier, and less on the collector

side. Thus a potential has to develop along the tube to compensate this effect, being higher at the emitter side and lower at the collector side. In other words, part of the potential drop takes place at the barrier as well as at the electrodes. For the limiting case of an insulating barrier, the whole potential drop V_{bias} occurs at the barrier. In the present calculations we have considered electrons flowing through an infinite tube, a segment of which (44 rings) is modified by disorder. Two planar infinite parallel metallic plates perpendicular to the tube are located at the ends of the segment, in order to electrostatically shield the semi-infinite electrodes.

One way to model disordered nanotubes is to add a random potential at every site. The distribution of potential values can be simply taken as equiprobable in the range $-\varepsilon/2 < V < \varepsilon/2$, ε being the disorder strength. When such a potential is added to the Hamiltonian, part of the potential drop takes place along the disordered region, and increases as the degree of disorder increases. Fig. 1 shows examples of the calculated self-consistent potential drop along a 5.3 nm long (5,5) nanotube having three different degrees of disorder for a bias of 4 V between the emitter and collector. The potential value was averaged over the 10 atomic rings nearest to the translational coordinate. Similar potential profiles were reported experimentally [11]. The argument proposed for the different slope of the potential drop as a function of the density of defects bases on experimental observation is in agreement with our calculation results.

Disorder strength is rather difficult to measure experimentally, and can be characterized by the electric current, a directly measurable quantity. We thus plot results of potential drop along the structure as a function of the total current, for different random potentials (Fig. 2). If the disorder is increased, the potential profiles become increasingly inhomogeneous and far from the linear shapes shown in Fig. 1. Therefore, only disorder degrees smaller than 8 V (for a 5.3 nm long structure) have been studied here. The maximum available drop of 4 V ($=V_{\text{bias}}$) would show up as a 3 V drop if the profile were linear and averaged as in Fig. 1, and would correspond to zero current. The highest available current for the structure is 9.4 ($2e^2V/h$), in the absence of disorder, which corresponds to 0 potential drop (at 4 V bias, conduction takes place through more than two subbands; biases smaller than $\sim$1 V, in absence of disorder, would yield a current of $2V_{\text{bias}}2e^2/h$). For the simulated range of currents in Fig. 2, the average of the potential drop (solid line) shows some curvature. The factors determining the curvature degree require further analysis, and are out of the scope of this paper.

Potential drop profiles due to disorder are homogeneously distributed along the disordered region. We can, nonetheless, study what happens if the scattering is produced in a controlled way, for instance, by making a heterostructure with tube sections of different helicities. We study the case of

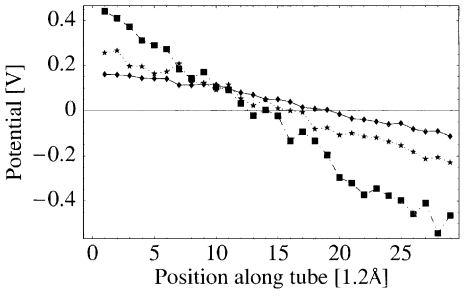


Fig. 1. Examples of self-consistent potential averaged over the 10 closest atomic rings around the longitudinal position, for three particular potentials with disorders degree $\varepsilon = 3$, 5 and 7 V (◆, ★, ■) respectively. The applied bias is 4 V in the three cases, and the length of the (5,5) tube is 5.3 nm.

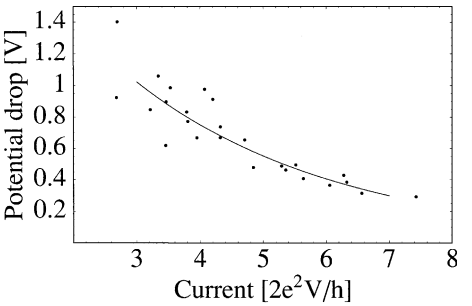


Fig. 2. Total potential drop (of the 10-ring averaged potential) along the disordered segment, shown vs. current, for a set of particular cases, together with their average curve (—).

a (6,6)(12,0)(6,6) straight junction containing 10 atomic rings in the (12,0) section. Both (6,6) and (12,0) tubes are metallic. However when matched together a gap is formed from about -1.5 to 1.5 eV around the Fermi level [4], due to the different angular momentum of the available electrons at this energy in the two parts ($L = 0$ at the (6,6) and $L = 4$ at the (12,0)). Therefore, for the heterojunctions considered, electrons with $L = 0$ tunnel between the electrodes, with a very small probability that depends on the length of the (12,0) region. At the same time, some $L = 4$ states are bound in the (12,0) segment, since they cannot escape to the electrodes (in order to allow these to be occupied by electrons in the self-consistent procedure, some inelastic scattering broadening of these states was assumed [12]. Fig. 3 shows an example of the self-consistent potential along this structure for a 5 V bias. The (12,0) segment goes from $X = 12$ to $X = 21$, where X denotes the atomic ring along the tube. Most of the potential drop takes place near these two interfaces and in the contacts. The total potential drop along the structure at this bias is about 25% of the total bias.

The current induced potential drop along the structure implies that the current vs. bias characteristics of the device are different than just the integral of the transmission at 0 bias. In Fig. 4 we show the actual current as a function of bias, together with the integral of the 0 bias transmission. The effect of the potential drop is to reduce the current about 50% of what a no-drop profile would yield.

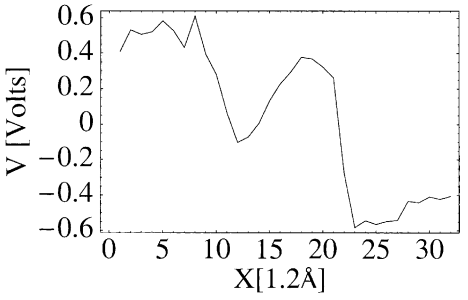


Fig. 3. Potential profile for the (6,6)(12,0)(6,6) metal–metal–metal heterostructure under 5 V applied bias (see explanations in text).

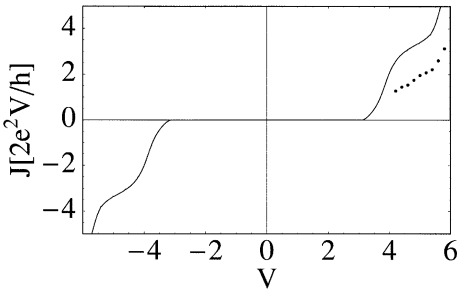


Fig. 4. Current intensity, $J(V)$, obtained for the heterostructure from the zero bias conductance (—), actual values of $J(V)$ when the potential along the structure is self-consistently calculated for each bias (•).

4. Conclusions

We have studied the self-consistent potential drop profile along carbon nanotube devices when a current is flowing, both for disordered and ordered (heterostructure) types of scattering defects. A Green function formalism has been shown, extending the self-consistent procedure to non-equilibrium situations. The self-consistent profile is a function of the applied bias. For the disordered potential case we find a roughly linear potential drop along the structure. The total potential drop as a function of disorder (characterized by current) shows a non-linear component. When scattering is produced by ordered structures, like a metal–metal–metal heterostructure, potential drop is shown to mostly take place at the interfaces between different helicities. The potential drop profile affects the $I(V)$ characteristics of the structure in an important degree. Our study shows that just a 0 bias transmission curve is not enough to define the $I(V)$ characteristics of nanotube junction devices. We have shown how these characteristics can be calculated. The recently demonstrated possibility to experimentally measure potential profiles 'in situ' [11] is expected in the near future to allow direct comparison with calculations.

Acknowledgements

N.M. acknowledges Prof. J.P. Lu of UNC for support and helpful comments, and NASA-Ames for usage of computing facilities.

References

[1] M.S. Dresselhaus, G. Dresselhaus, P.C. Eklund, Science of Fullerenes and Carbon Nanotubes, Academic Press, London, 1995.
[2] S.J. Tans, A.R.M. Verschueren, C. Dekker, Nature 393 (1998) 49–52.
[3] Z. Yao, H.W.Ch. Postma, L. Balents, C. Dekker, Nature 402 (6759) (1999) 273–276.
[4] L. Chico, L.X. Benedict, S.G. Louie, M.L. Cohen, Phys. Rev. B 54 (1996) 2600.
[5] P.L. Pernas, A. Martin-Rodero, F. Flores, Phys. Rev. B 41 (1990) 8553.
[6] J. Han, Chem. Phys. Lett. 282 (2) (1998) 187–191.
[7] J. Han, L. Yang, N. Mingo, to be published.
[8] F. Guinea, C. Tejedor, F. Flores, E. Louis, Phys. Rev. B 28 (1983) 4397.
[9] F.J. Garcia-Vidal, J. Merino, R. Perez, J. Ortega, F. Flores, Phys. Rev. B 50 (1994) 10537.
[10] N. Mingo, F. Flores, Surf. Sci. 395 (1998) 342.
[11] A. Bachtold, M.S. Fuhrer, S. Plyasunov, M. Forero, E.H. Anderson, A. Zettl, P.L. McEuen, Phys. Rev. Lett. 84 (2000) 6082.
[12] J. Cerda, M.A. van Hove, P. Sautet, M. Salmeron, Phys. Rev. B 56 (24) (1997) 15885–15899.